Remote Sensing in Ecology and Conservation
Open Access
ZSL

RESEARCH ARTICLE

Hyperspectral species maps and LiDAR-based structured population models show future forest fire frequency may compromise forest resilience

Jessica McLean[1], Tommaso Jucker[2], Alice Rosen[1], Sean M. McMahon[3] & Roberto Salguero-Gómez[1]

[1]Department of Biology, University of Oxford, Oxford, UK
[2]School of Biological Sciences, University of Bristol, Bristol, UK
[3]Smithsonian Environmental Research Center, Edgewater, Maryland, USA

Keywords
boreal forest, disturbance, fire ecology, integral projection model (IPM), passage time, remote sensing

Correspondence
Jessica McLean and Roberto Salguero-Gómez, Department of Biology, University of Oxford, Oxford, UK. Tel: +44 (0) 1865271188; E-mail: jessicamclean302@gmail.com and rob.salguero@biology.ox.ac.uk

Funding Information
This work was supported by Natural Environment Research Council (NE/X013766/1).

Editor: Prof. Mat Disney
Associate Editor: Dr. Wang Li

Received: 23 July 2025; Revised: 7 December 2025; Accepted: 17 December 2025

doi: 10.1002/rse2.70057

Remote Sensing in Ecology and Conservation 2026;**12** (4):577–592

Abstract

Forest disturbances are accelerating biodiversity loss and altering tree productivity worldwide. Post-disturbance recovery time, a component of resilience, is critical for identifying vulnerable areas and targeting conservation but varies with environmental conditions. Monitoring recovery at scale requires tracking tree dynamics, yet traditional ground-based approaches are resource-intensive. We present a pipeline to parameterize integral projection models (IPMs) using LiDAR data and hyperspectral-based species maps to assess post-fire recovery across large, forested areas. Focusing on the fire-adapted *Picea mariana*, we model passage times to reproductive heights and life expectancy under different fire regimes as indicators of recovery time. To do this, we combined hyperspectral-based species maps and LiDAR-based crown heights to track individual tree survival and growth at the Caribou-Poker Creek Research Watershed (BONA) from 2017 to 2023. We incorporated fire history, aspect, slope, elevation and surrounding canopy height into our models and found partial support for their expected effects on survival and growth. Once accounting for topography and competition, we estimated passage times to reproductive maturity (11–22 years). Life expectancy in the absence of fire is shortest on North-facing slopes with recent fire (581 years). Sensitivity analyses highlight fire history and aspect as key modulators of population resilience, with elevation exerting strong influence on life expectancy across all conditions. Our results demonstrate that remotely sensed IPMs can effectively quantify forest recovery at scale, revealing that in some contexts, stands of *P. mariana* may not recover between fire disturbances. We discuss the implications of these findings for advancing modelling of resilience and highlight both the challenges and opportunities of using LiDAR and hyperspectral data to build demographic models for forecasting forest dynamics.

Introduction

Forest disturbances, such as pests, drought and fires affect the composition and function of forests (Canelles et al., 2021; Hammond et al., 2022; Roces-Díaz et al., 2022). Predicting resilience, the ability for tree populations to absorb and respond to such disturbances (Holling, 1973; Pimm, 1984), however, is challenging. The characteristics of resilience, including resistance to the disturbance, potential recovery time and potential displacement to an alternative stable state (*sensu* May, 1977), can be specific to a species and given environmental conditions. Demographic analyses offer a robust way to translate the vital rates (e.g., survival, growth) of individual trees in particular conditions into estimates of demographic resilience to disturbances (Capdevila et al., 2020). However, demographic data on individuals are difficult to acquire over large spatial domains, further challenging

© 2026 The Author(s). *Remote Sensing in Ecology and Conservation* published by John Wiley & Sons Ltd on behalf of Zoological Society of London. This is an open access article under the terms of the Creative Commons Attribution License, which permits use, distribution and reproduction in any medium, provided the original work is properly cited.

our ability to link disturbances that can span regions to projections emerging from the collective response of individual trees (Battison et al., 2024; Ma et al., 2023; Rosen et al., 2025; Stovall et al., 2019).

Remote sensing technology, including hyperspectral imagery and light detection and ranging (LiDAR), has accelerated the monitoring of forest disturbances (Cavendar-Bares et al., 2020; Fassnacht et al., 2024). Indeed, repeat airborne LiDAR acquisitions can now be used to track changes in tree canopies over thousands of hectares at a very high spatial resolution (1–4 m^2) (Jucker, 2022). While aerial laser scanning has been previously utilized to understand canopy-level effects of disturbances (Choi et al., 2023; Cushman et al., 2021), improvements in individual tree detection methods (Cao et al., 2023; Dalponte & Coomes, 2016) have opened the opportunity to track trees through time (Battison et al., 2024; Beese et al., 2022; Duncanson & Dubayah, 2018). The advances in LiDAR technology, uptake and availability have led to greater repeatability and increased spatial coverage, which overcomes the major time and labour constraints of classical approaches to collecting field data (Fischer et al., 2025; Salguero-Gómez & Gamelon, 2021). Furthermore, the differences in the reflectance spectra of different tree species can be used to identify specific populations, especially in low-diversity landscapes (Dalponte & Coomes, 2016; Scholl et al., 2020; Weinstein et al., 2024). The large sample sizes resulting from remote sensing approaches (e.g., combining laser scanning for tree measurements and hyperspectral for species mapping) offer data for analyses at the spatial scales of many disturbance events.

Structured population models parametrized with demographic LiDAR data can estimate how disturbances affect vital rates like survival, growth and reproduction. Indeed, ecologists use these models to examine the effects of habitat fragmentation (Zambrano & Salguero-Gómez, 2014), pathogens (Needham et al., 2016), or climate change (Kunstler et al., 2021) on forest dynamics. In their standard version, integral projection models (IPMs hereafter; Easterling et al., 2000; Ellner & Rees, 2006), a form of structured population model, describe the temporal changes in population distribution of individuals as a function of a continuous trait that predicts vital rates (Merow et al., 2014). Historically, tree-structured population models (including IPMs) have used diameter at breast height (DBH) to predict vital rates (Metcalf et al., 2009; Needham et al., 2016, 2018; Ohse et al., 2023; Salguero-Gómez et al., 2015). However, LiDAR-derived traits, like tree height, can also predict productivity, competition and mortality (Jucker et al., 2017; Maynard et al., 2022; Zuleta et al., 2022). Additionally, as IPMs can incorporate a/biotic factors in their regression-based vital rate models (Ellner & Rees, 2006; Merow et al., 2014), they can estimate population responses to disturbances. Still, the fields of remote sensing, using hyperspectral and LiDAR data, and population ecology, using IPMs, have independently investigated the effect of disturbances on forests. Combining these approaches offers a way to parameterize the detail of a population model with the spatial extent of remote sensing (Rosen et al., 2025).

In boreal forests, the increasing frequency of the historically regular wildfires (Chapin et al., 2006; MacDonald et al., 1991) is compromising their ecological integrity (Palm et al., 2022; Tollefson, 2024), even among fire-adapted tree species (Whitman et al., 2019). Here, we focus on black spruce, *Picea mariana* (Mill.) B. S. P., which dominates North American boreal forests. The conifer species' dominance is mainly attributed to high post-fire replacement, as *P. mariana* has semi-serotinous cones (Fryer, 2014). However, shorter fire intervals limit time to reproductive maturity, limiting recruitment (Brown & Johnstone, 2012; Johnstone et al., 2020). Interior Alaska's historical fire interval was every 100–-150 years (Fryer, 2014), aligning with peak *P. mariana* cone production at 100–200 years (Splawinski et al., 2022). Now, intervals can be as short as 50 years (Buma et al., 2022). When *P. mariana* recruitment is low, wind-dispersing species, like white spruce (*Picea glauca*) and Alaskan birch (*Betula neoalaska*) establish instead (Johnstone et al., 2020), altering carbon and nutrient cycling (Melvin et al., 2015) and understory vegetation (Hart & Chen, 2006). The regeneration of *P. mariana* is related to its height, as taller individuals produce more cones (Simpson & Powell, 1981). In the absence of fire, mortality mainly results from windthrow and permafrost-related waterlogging, both reducing height (Dearborn et al., 2021; Elie & Ruel, 2005). These traits make *P. mariana* ideal to model its vital rates as a function of height in IPMs (Easterling et al., 2000).

Here, we quantify the impacts of fire on the survival and growth of black spruce, *Picea mariana*, via IPMs parameterized with LiDAR data and a hyperspectral-based species map (Fig. 1). Across 26 km^2 of Alaskan boreal forest, we examine how forest patches with different fire history inform which fire intervals are in/compatible with post-disturbance recovery. We test the following hypotheses:

H1

Lower surrounding canopy height (SCH), lower elevation and less steep slopes will be favourable for individual survival and growth. Such conditions may support survival and growth because of the decrease in competition (Carleton & Wannamaker, 1987), increase in temperature (Fryer, 2014), and increase in ground stability (Nicoll et al., 2005), respectively. To test H1, we constructed regression models of survival and growth, using height and environmental variables as predictors.

© 2026 The Author(s). *Remote Sensing in Ecology and Conservation* published by John Wiley & Sons Ltd on behalf of Zoological Society of London.

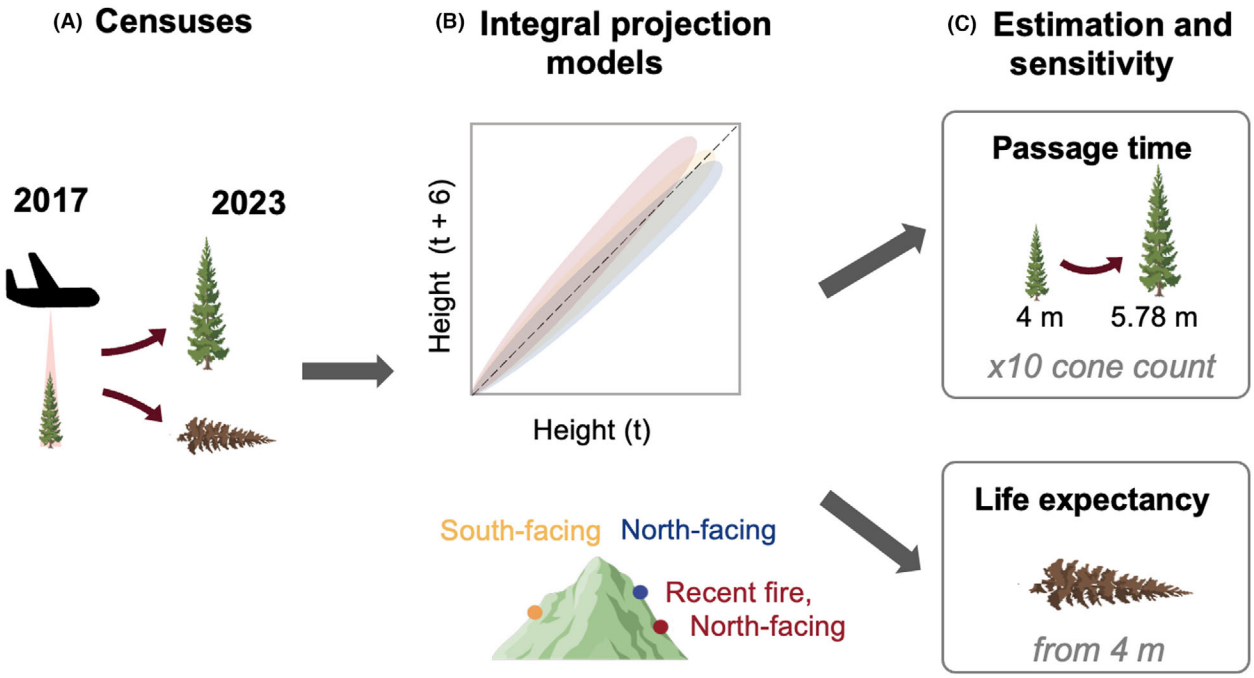


Figure 1. An overview of the integration of RGB, hyperspectral, and LiDAR (light detection and ranging) data acquisition implemented here to estimate the time to a target height and life expectancy in a forest population of *Picea mariana*. (A) Here, to model the time required for boreal forests to recover from fire, we located *P. mariana* using Weinstein et al.'s (2024) species map, which used RGB imagery and hyperspectral imagery to train a machine learning model to detect individual trees in the upper canopy and identify them to species level. Next, we quantified the survival and growth of 42,816 individuals of *P. mariana* using LiDAR censuses between 2017 and 2023. (B) We then integrated the models of survival and growth into integral projection models (IPMs), explicitly including environmental descriptors of fire history and terrain aspects. We estimated (C) passage time, defined as the time to grow from 4 m to 5.78 m, which is equivalent to a 10-fold increase in cone count (Simpson & Powell, 1981), and mean life expectancy. The faster *P. mariana* can increase cone count, the more likely the stand will recover and recruit new individuals post-fire. For both passage time and life expectancy, we examined how sensitive the life history traits are to small perturbations in key environmental drivers for each of the three IPMs: elevation, slope steepness, and surrounding canopy height.

H2

The longest passage time will occur in stands without recent fire history on North-facing slopes, since trees in these patches likely experience higher density dependent competition combined with limited light availability (Carleton & Wannamaker, 1987; Nath & Ni-Meister, 2021; Van Cleve et al., 1986). To test H2, after integrating the IPMs with the regression models chosen from testing H1, we calculated passage time, a proxy of resilience that relates to the speed of recovery of a population post-disturbance (Capdevila et al., 2022).

H3

Life expectancy should be longest on slopes with recent fire history because the recent fire likely cleared the canopy (*P. mariana* is highly flammable; Cronan et al., 2012), replaced by new recruits. To test H3, we used the same IPMs from testing H2 to also calculate life expectancy, another proxy of resilience that relates to the speed of recovery of a population post-disturbance (Capdevila et al., 2022).

H4

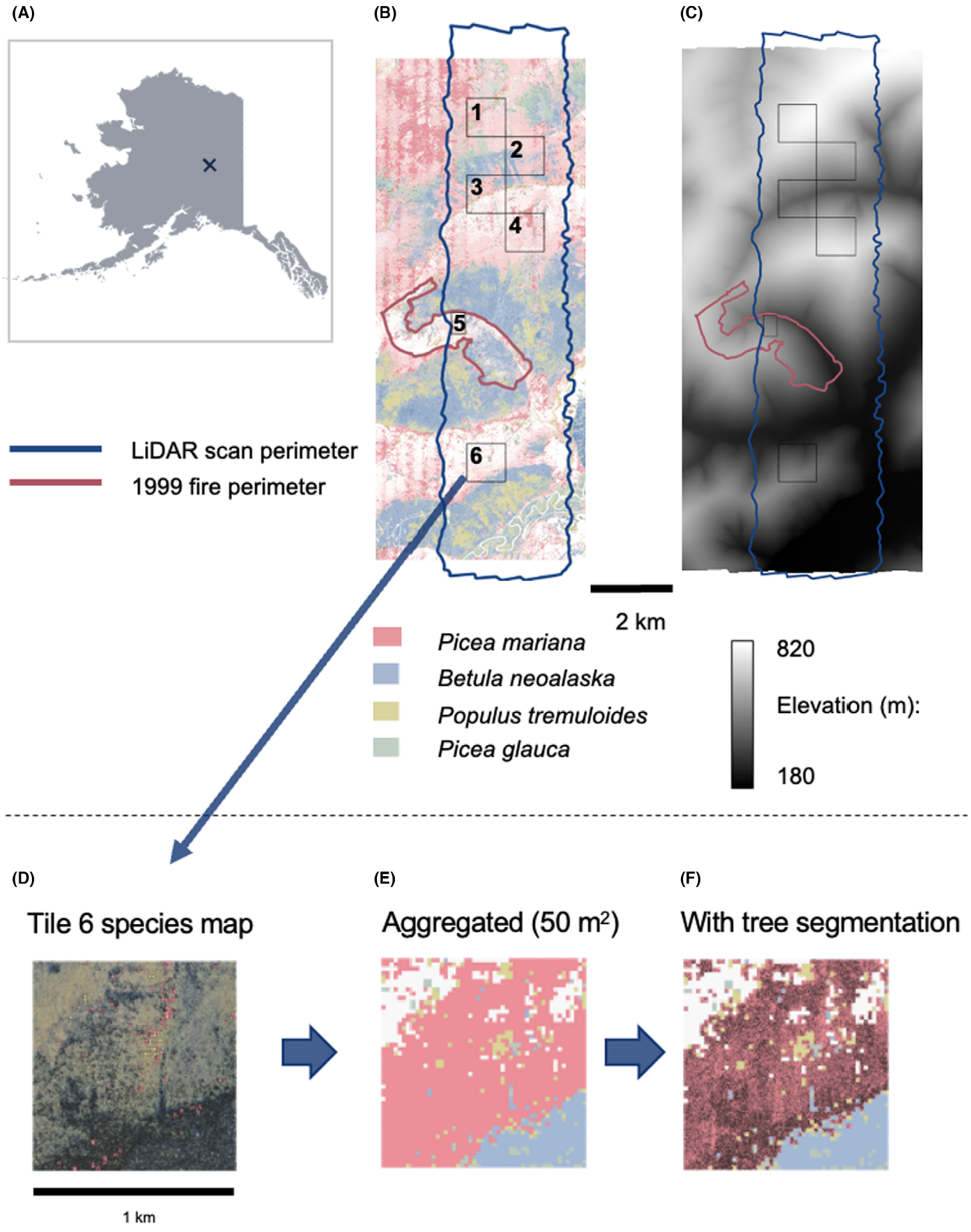
Passage time and life expectancy will be most sensitive to elevation where there is increased light availability at higher elevations. Taller *P. mariana* individuals have been found at higher elevations on South-facing slopes (Nath & Ni-Meister, 2021). To test H4, we performed a sensitivity analysis of passage time and life expectancy in relation to elevation, slope steepness and SCH.

Materials and Methods

Site selection with remote sensing data

To understand the resilience of *Picea mariana* in different environmental conditions, we built IPMs parameterized with LiDAR-based height change and hyperspectral-based species

© 2026 The Author(s). *Remote Sensing in Ecology and Conservation* published by John Wiley & Sons Ltd on behalf of Zoological Society of London.



© 2026 The Author(s). *Remote Sensing in Ecology and Conservation* published by John Wiley & Sons Ltd on behalf of Zoological Society of London.

Figure 2. We brought together data from multiple sources, including a machine learning-based species map reliant on RGB and hyperspectral data, and satellite fire history, to locate *Picea mariana* individuals across a topographic gradient for model parameterization. Maps of the LiDAR scan perimeter (dark blue) in 2017 and 2023 over different maps. In the (A) Alaska map, the LiDAR scan location is marked with an 'X' at the Caribou-Poker Creek Research Watershed (BONA), near Fairbanks. (B) The species map shows the upper canopy species predictions (Weinstein et al., 2024) and (C) the elevation map shows the topography (Fischer et al., 2024) at the BONA site. The six tiles (numbered in B) within the scan perimeter indicate the selected areas that were examined in 2017 and 2023. Note: tile 5 was experimentally burnt in 1999 (FROSTFIRE; Hinzman et al., 2003) and was cropped to only include trees within the fire patch (300 m × 400 m) while the other five remained 1 km × 1 km. The blue rectangle shows the overlapping LiDAR scans in 2017 and 2023. The 1999 fire perimeter (red polygon) is derived from satellite imagery (Alaskan Wildland Fire Information Map Series). Zooming in on tile 6, we illustrate the individual species labelled tree crowns over (D) RGB imagery based on analyses by Weinstein et al. (2024). From the species labelled tree crown map, we then (E) aggregated to a 50 m^2 resolution with each grid cell labelled by species dominance, and (F) overlayed the LiDAR-based tree crown segmentation and filtered for trees only in *P. mariana*-dominated grid cells (pink).

maps. We used National Ecological Observatory Network data (NEON, 2025a, 2025b, 2025c) at the Caribou-Poker Creek Research Watershed (BONA site, Alaska, USA) acquired in 2017 and 2023 (See Table S1 in Supplementary Materials for LiDAR scan characteristics). By remotely detecting survival and growth of individuals we parameterized IPMs (Section 1) and estimated passage time and life expectancy (Section 2). To select areas within the 26 km^2 scan overlap (Fig. 2B and C), we aimed to include patches with different fire history (either within the FROSTFIRE 1999 experimental fire patch, or the last fire occurred before 1940; Bureau of Land Management, n.d., Hinzman et al., 2003), elevations and aspect that are dominated by *P. mariana* (Fig. 2 tiles 1–6, totalling 5.5 km^2). See Section 1 in the Supplementary Materials for full details about the tile selection criteria.

To locate *P. mariana*-dominated areas to track survival and growth in, we utilized a hyperspectral-based species map. The upper canopy of the BONA site includes Alaskan birch (*Betula neoalaskana*), white spruce (*Picea glauca*) and trembling aspen (*Populus tremuloides*). The former two species are wind-dispersing species that have previously outcompeted *P. mariana* when given inadequate recovery time (Johnstone et al., 2020). Briefly, Weinstein and colleagues used 1 m^2 resolution hyperspectral reflectance and geolocated field data to build a machine learning model that assigned species-IDs to tree crowns segmented with 10 cm^2 resolution RGB imagery (Weinstein et al., 2020, 2024). The BONA site had an 82% 'micro-accuracy' (indication of performance in labelling the more common species), which is the third highest site score out of 23 NEON sites (see tab. 2 of Weinstein et al., 2024).

Building IPMs with LiDAR data

Estimating survival and growth from individual tree height

To estimate survival and growth, we measured height change between 2017 and 2023 using crown polygons segmented from a 2017 canopy height model (CHM) within *P. mariana*-dominated areas of the hyperspectral-based species map. From the Weinstein et al. (2024) hyperspectral-based species map, we aggregated tiles to 50 m^2 grid cells labelled by species dominance (Fig. 2E), overlaid the 2017 CHM crown segmentation (see below), and retained trees within *P. mariana*-dominated cells (Fig. 2F). We included only crowns $\geq$3 m^2, ensuring height estimates were informed by at least four CHM pixels and minimizing errors due to CHM misalignment. We set the minimum individual tree height to 4 m because the ability to accurately detect the crowns of smaller trees is limited in general with LiDAR, as these are occluded by larger neighbours (Battison et al., 2024; Dalponte & Coomes, 2016; Cao et al., 2023; see Table S1 for LiDAR scan statistics). The final dataset contained 42,816 individuals over 4 m tall in 2017 (mean height = 6.93 m, mean crown area = 8.01 m^2).

To delineate individual tree crowns, we used the Dalponte and Coomes (2016) segmentation algorithm, which operates faster than other options (Cao et al., 2023). The algorithm identifies local maxima, expands the crowns based on a given window size, and segments crown boundaries. We used a 1 m resolution CHM generated with the 'highest' algorithm, a data product from Fischer et al. (2024), which is designed to reveal upper canopy treetops. See Section 2 of the Supplementary Materials for full details about the algorithm fine tuning and how accuracy was assessed. Briefly, we found 24.4% of autosegmented trees with a crown area of at least 3 m^2 overlapped with manually segmented trees (211 out of the 863 manually segmented trees in a 150 m × 500 m strip).

To measure tree height as a proxy for survival and growth, we extracted the maximum CHM height within each tree polygon. We classified an individual as dead if its height decreased by $\geq$50% between 2017 and 2023. While past studies applied a 30% threshold, we used a

© 2026 The Author(s). *Remote Sensing in Ecology and Conservation* published by John Wiley & Sons Ltd on behalf of Zoological Society of London.

more conservative threshold to account for inter-census variability in CHM-derived height (Battison et al., 2024; Duncanson & Dubayah, 2018; Ma et al., 2023). We used CHMs calculated from the 'spikefree' algorithm from Fischer et al.'s (2024) data products, designed to make CHMs acquired at different pulse densities (>2 pulses per m^2; See Fig. 2 of Fischer et al., 2024) directly comparable (See Table S1). The CHMs were produced based on the Digital Terrain Model of the same year (DTM; Fischer et al., 2024). See Section 3 of the Supplementary Materials for full details about the height change, mortality rate observed, comparison to NEON ground data and canopy height maps.

We carried out spatial analyses and statistical modelling on R version 4.3.2 (R Core Team, 2023). We implemented the spatial data processing using the *lidR* (Roussel, 2025; Roussel et al., 2020), *sf* (Pebesma, 2018) and *terra* R packages (Hijmans et al., 2024) for individual tree crown segmentation, vector data (tree crowns) and raster data (CHMs and DTMs), respectively.

Quantifying environmental drivers

We quantified each environmental driver to investigate (H1–H3) their effect on survival and growth. Recent fire was a binary factor, with 'no' for individuals outside of the 1999 fire patch. From the 2017 DTM (Fischer et al., 2024), we extracted the mean elevation for each tree and derived aspect and slope maps using the R *terra* package (Hijmans et al., 2024). For aspect, we cosine-transformed the map from a 360° scale to −1 to 1 scale to focus on North and South aspect, respectively (Beese et al., 2022). Lastly, we measured the Surround Canopy Height (SCH; Battison et al., 2024; Krause & Lemay, 2023), which is the average height within a 15 m buffer around each tree. Our findings were robust to the choice of SCH radius (see Section 4 of the Supplementary Materials).

To also consider if height changes may be due to differences between the point density of the scans in 2017 and 2023, we determined the Relative Change in Point density (RCP, Eq. 1) for each individual tree. The average point density in 2023 was approximately fourfold higher than in 2017 (20.1 pts/m^2 in 2023, 5.12/m^2 in 2017; Fischer et al., 2024). To measure RCP, we used a relative metric because higher point densities plateau to a stable height measurement (Hawryło et al., 2024). A description of all environmental covariates derived from remote sensing data is found in Table S2.

$$\mathrm{RCP} = \frac{(\text{point density } 2023 - \text{point density } 2017)}{\text{point density } 2017} \quad (1)$$

Selecting and integrating vital rate models into IPMs

To estimate passage time and life expectancy, we parameterized IPMs (see Coulson, 2012; Rees et al., 2014; Ellner et al., 2016 for an introduction). IPMs are demographic models that describe changes in the structure of a population along a continuous trait (here, tree height) in discrete time. The integration of survival and growth models into the IPM framework produces a two-dimensional P kernel (Ellner et al., 2016). IPMs often contain an F kernel, which describes the recruitment of new individuals to the population (Easterling et al., 2000; Ellner & Rees, 2006). However, only survival and growth are necessary to test our hypotheses (but see Discussion; Merow et al., 2014; Metcalf et al., 2013). Our P kernel tracks progression of the structure of a *P. mariana* population, n, between a range of possible heights, from the lower (L) to upper (U) bounds of the integral defined by Equation 2, to the next time step in the censused data (here $t+6$ years):

$$n(y, t+6) = \int_L^U P(y,x)n(x,t)\,dx \quad (2)$$

The P kernel (Eq. 3) is composed of the s survival function (probability of survival for a given height x in time t) and the g growth function (the probability that a tree of a given height x in time t will grow to a given height y in $t+6$). For more details about IPM midpoint integration, including determination of the bounds of the P kernel integral (Eq. 2) and choice of meshpoints, see Section 5 of the Supplementary Materials.

$$P(y,x) = s(x)g(y,x) \quad (3)$$

Before model construction, we checked for multicollinearity in the model predictors. We calculated Pearson's correlation coefficient (ρ) between all model predictors to exclude one of the two variables involved in pair-wise correlations raising $|\rho| > 0.6$, following Beese et al. (2022). The highest correlation coefficient was below this threshold though: between slope steepness and elevation ($\rho = -0.56$) and SCH and height ($\rho = 0.58$) (See Fig. S7).

To test H1 on the effects of environmental drivers on survival and growth and to select the models for the IPMs (H2–H4), we started with the most complex additive models given our hypotheses. We modelled survival probability in the examined period as a binomial logistic regression of height (x, log-transformed; Eq. 4) and we modelled growth as the change in height of surviving individuals (Eq. 5). The final models were polynomial (logistic, for survival) regressions, including a quadratic

 © 2026 The Author(s). *Remote Sensing in Ecology and Conservation* published by John Wiley & Sons Ltd on behalf of Zoological Society of London.

term for height, an intercept shift for individuals on North-facing slopes (*North*) or individuals inside a stand burnt in 1999 (*Fire*) and four environmental covariates (*Elevation*, *Steepness*, *RCP* and *SCH*). For each environmental covariate, we used the mean value across the dataset (e.g., $Elevation_s$; See Section 8 of the Supplementary Materials) multiplied by its slope estimate, indicated by the hat (e.g., $\widehat{e}_s$). Full summaries of the selection process and model estimates can be found in the Supplementary Material (Sections 9–11). To account for uncertainty in LiDAR-derived height, we quantified the error in the mean growth function (ε) following Clark (2003), as detailed in Section 11 of the Supplementary Materials. We conducted ANOVA analyses and the results of the *F*-test for the environmental drivers of growth were summarized using the library 'report' (Makowski et al., 2025).

$$logit[s(x)] = a + b_s x + c_s x^2 + North_s + Fire_s + Elevation_s\widehat{e}_s + Steepness_s\widehat{s}_s + RCP_s\widehat{RCP}_s + SCH_s\widehat{SCH}_s \quad (4)$$

$$g(y,x) = a_g + b_g x + North + Fire + Elevation_g\widehat{e}_g + \widehat{s}_g + RCP_g\widehat{RCP}_g + SCH_g\widehat{SCH}_g + \varepsilon \quad (5)$$

We altered the recent fire history and aspect conditions in the survival and growth models when we integrated the IPMs to compare their outputs. The same survival and growth functions were used to build all three IPMs (Eqs 4 and 5 integrated as in Eq. 3) but differed in intercepts for fire history and aspect. The resulting three IPMs were two North-facing (1) with or (2) without recent fire history, and one additional IPM with (3) South-facing without recent fire history. We did not parameterize an IPM with recent fire and South-facing slope, as this combination of conditions does not exist at the BONA site during the monitored period. The final integrated IPM kernels are also presented in the Supplementary Material in Section 12. Because of the 6-year interval between censuses, the outputs of passage time and mean life expectancy were multiplied by six, so the final outputs are in the units of years.

Calculating passage time and life expectancy from IPMs

To test our hypothesis (H2) that the longest passage times occur on North-facing slopes without recent fire history, we compared the IPM-derived passage times, that is, the time elapsed for individuals of a given height to achieve a target height (Merow et al., 2014). Our passage time of interest was between 4 m, the shortest tree height in our dataset extracted from the 2017 CHM, to 5.78 m, the target height corresponding to a 10-fold increase in cone production compared with a 4 m tall individual tree, according to the height to cone count regression modelled by Simpson and Powell (1981). Taller trees may have a higher chance at self-replacement (Simpson & Powell, 1981; Viglas et al., 2013). Using 5.78 m as the target height also prevents extrapolation outside the maximum height observed in the fire patch (See Section 13 of the Supplementary Materials). To estimate passage time, we initialized a population vector with 1,000 individuals in the starting height class and applied the *P* kernel iteratively until the population mean reached the target height, allowing for linear interpolation. We performed 1,000 bootstraps, each sampling 95% of the data, to estimate standard deviation.

To test the hypothesis (H3) that life expectancy is highest on slopes with no recent fire history, regardless of aspect, we used the *Rage R* package (Barks et al., 2023; Jones et al., 2022). Life expectancy was defined as the mean age at death for individuals, conditional on having reached 4 m tall, the shortest height observed with LiDAR in this study. Because no fires occurred between censuses, these estimates reflect life expectancy in the absence of fire. To understand the variance of mean life expectancy between environmental conditions, we bootstrapped 95% of the individual trajectories 1,000 times. We calculated standard errors from these bootstraps to detect significant differences in mean life expectancy and performed a one-way ANOVA followed by a post hoc HSD Tukey test.

For both life expectancy and passage time, we conducted a sensitivity analysis to test (H4) that these traits are most sensitive to elevation, with higher sensitivity on North-facing slopes. For each of the three IPMs, we perturbed the three environmental drivers (elevation, slope steepness and SCH) using the 'brute force' method (*sensu* Morris & Doak, 2002). We increased each parameter's slope coefficient by 1% individually and recalculated passage time and life expectancy. We then quantified sensitivity by comparing the new estimates with the original mean values of passage time and life expectancy.

Results

Environmental drivers of survival and growth

We found support for our hypothesis (H1) that certain environmental conditions would influence the survival and growth of individuals of *P. mariana*, but not always in the direction we expected (Table 1). It is worth noting that, in both models of survival and growth, the slope estimates are quite small for the overall regression slope, but that their significant differences and the Aikaike Information Criterion (AIC) comparison support their importance to the model in improving population

© 2026 The Author(s). *Remote Sensing in Ecology and Conservation* published by John Wiley & Sons Ltd on behalf of Zoological Society of London.

Table 1. All five environmental drivers examined in this study predict the survival and growth of *Picea mariana* individuals between 2017 and 2023, as shown by Odds Ratio calculations for survival (A) and by ANOVA analysis (B) for growth.

A Environmental driver	Std Ratio	95% CI
Aspect	0.431	[0.294, 0.622]
Slope steepness	0.816	[0.726, 0.918]
Elevation	1.296	[1.137, 1.477]
Recent fire	2.443	[1.227, 5.791]
Surround Canopy Height	4.680	[3.786, 5.838]

B Environmental driver	Df	*F* value	*P* value	95% CI
Aspect	1	3733.624	<0.001***	[0.08, 1.00]
Slope steepness	1	141.412	<0.001***	[2.47e-03, 1.00]
Elevation	1	11.679	<0.001***	[7.40e-05, 1.00]
Recent fire	1	194.488	<0.001***	[3.55e-03, 1.00]
Surround Canopy Height	1	3823.953	<0.001***	[0.08, 1.00]

Note: We calculated the environmental drivers in the same way for both models: elevation is the high above sea level (m) which we derived from the 2017 digital terrain model (DTM); slope steepness is the percentage change in the DTM, aspect is a binary variable of either North- or South-facing, again derived from the 2017 DTM; surround canopy height (SCH) is the average height of the canopy within a 15 m radius of the tree, which we derived from the 2017 canopy height model (CHM); and recent fire history was assigned to trees growing inside the 1999 fire patch, as provided by an Alaska Wildland Fire Information Map Series shapefile. Full model summaries including all model parameters and associated analyses can be found in the Supplementary Online Materials in Sections 9–11.
***$P < 0.001$.

forecasts (Tables S3-S9; Tables S4 and S7 for coefficient values for survival and growth, respectively). Regarding the odds ratio and ANOVA analyses, lower slope steepness (i.e., flatter terrain) has a positive effect on both survival (OR = 0.816, 95% CI = [0.726, 0.918]) and growth ($F_{1,42463} = 141.412$, $P < 0.001$; Eta2 (partial) = 0.0003, [0.0002, 1.00]). Contrary to our hypothesis, though, increases in elevation and SCH have a positive effect on both survival (Elevation: (OR = 1.296, 95% CI = [1.137, 0.918]; SCH: OR = 4.680, 95% CI = [3.786, 5.838])) and growth (Elevation: ($F_{1,42463} = 11.679$, $P < 0.001$; Eta2 (partial) < 0.001, [0.000, 1.000]); SCH: ($F_{1,42463} = 3823.953$, $P < 0.001$; Eta2 (partial) = 0.08, [0.080, 1.000])). Full odds ratio and ANOVA analyses for all parameters of the survival and growth models are available in the Supplementary Online Materials in Sections 9 and 10, respectively.

Passage time and sensitivity analysis

As we had expected (H2), the longest passage time occurs in stands without recent fire history on North-facing slopes. In Figure 3, the passage time from 4 m to the target height is the starting point of each line, with passage time decreasing as the starting height approaches the target height. Specifically, stands located on North-facing slopes without recent fire history have a passage time of 22.21 years (± 0.15 SD) from 4 m to the target height. The passage times from 4 m to the target height in other conditions are lower, with a passage time of 16.22 years (± 0.14) on South-facing slopes without recent fire history and 11.65 years (± 0.08) for sites with recent fire history on a North-facing slope.

We did not find support for our hypothesis (H4) that passage time would be most sensitive to elevation. Indeed, across all combinations of environmental conditions, increases in the elevation slope parameter correspond to shorter passage time, as mediated by its effects on survival and growth (Fig. 5A–C). However, passage time is most negatively sensitive to SCH, as mediated by its effect on growth (Fig. 5B). The negative sensitivity of passage time to perturbations across all environmental drivers is most extreme for the no recent fire and North-facing combination, followed by no recent fire, South-facing, and the least sensitivity in the recent fire and North-facing conditions.

Life expectancy and sensitivity analysis

Contrary to our third hypothesis (H3), life expectancy is estimated to be much longer in stands located on slopes without recent fire history, rather than with recent fire history. The conditions of recent fire on a North-facing slope result in a mean life expectancy of 581 years (± 1.80 S.E.), while no recent fire history stands on North- and South-facing slopes raise a mean life expectancy of 1,192 years (± 1.37) and 1,556 years (± 1.92), respectively (Fig. 4). The one-way ANOVA confirms a significant difference in the mean life expectancies between at least two of the groups ($F_{2,2997} = 82747.95$, $P < 0.001$; 95% CI [0.980, 1.000]). Furthermore, in the post hoc Tukey test, all possible comparisons between two groups are significantly different (adjusted *p*-values for each comparison < 0.050).

We found support for our fourth hypothesis (H4) that life expectancy should be highly sensitive to elevation. Indeed, elevation was the primary driver of life expectancy via its effects on growth across all environmental conditions (Fig. 5D–F). The negative sensitivity of life expectancy to perturbations across all environmental drivers is most extreme for the no recent fire and

© 2026 The Author(s). *Remote Sensing in Ecology and Conservation* published by John Wiley & Sons Ltd on behalf of Zoological Society of London.

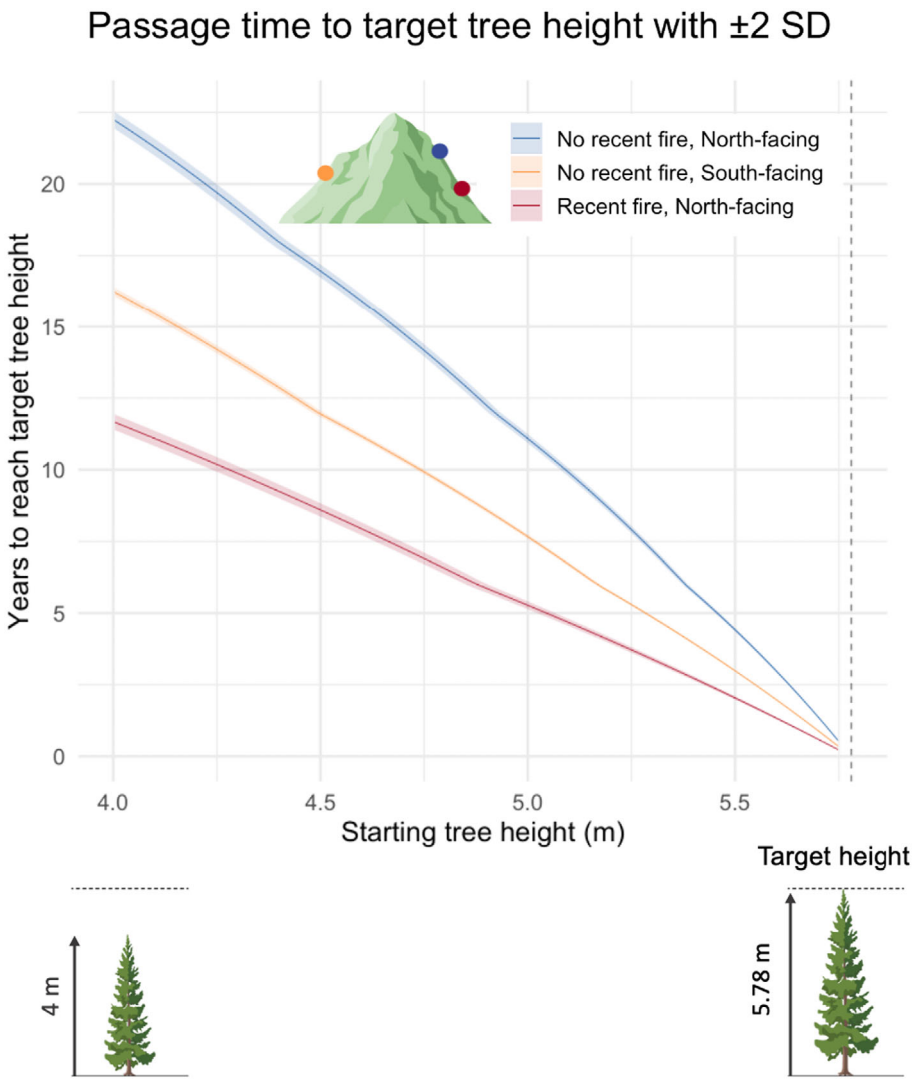


Figure 3. Trees with recent fire history on North-facing slopes have the fastest recovery time to heights of higher chances of self-replacement. The passage times of an individual of *Picea mariana* from 4 m tall to the target height of 5.78 m (black vertical line) informs the time required for the boreal forest to recover before fire returns as ten times increase in cone count. The target height is represented as the black vertical line on the right of the graph, as well as the horizontal line above each tree at the bottom of the figure. Across all combinations of fire history and aspect conditions, as the starting tree height gets closer to the target height, the years to reach the target height decrease. The shaded areas correspond to 2 S.D. around the mean passage time.

South-facing combination, followed by no recent fire, North-facing and the least sensitivity in the recent fire and North-facing conditions.

Discussion

Anthropogenic disturbances, including pests, drought and fires, threaten tree longevity (Cobb et al., 2017) and global forest productivity (Hogan et al., 2024; Morin et al., 2018). To maintain forest biodiversity and ecosystem services (Brockerhoff et al., 2017; Mo et al., 2023), we urgently need to identify which forests are least resilient – and to what disturbances – to inform management strategies (Ibáñez et al., 2019; Thorogood et al., 2023). However, the survival and growth rates of trees can vary greatly among and within species (Bialic-Murphy et al., 2024; Drobyshev et al., 2013) and across environmental conditions (McMahon et al., 2010; Ohse et al., 2023). To overcome this challenge, we parameterized LiDAR-based integral projection models (IPMs; Easterling et al., 2000) to examine the drivers of passage time and life expectancy of *Picea mariana*, a species vulnerable

© 2026 The Author(s). *Remote Sensing in Ecology and Conservation* published by John Wiley & Sons Ltd on behalf of Zoological Society of London.

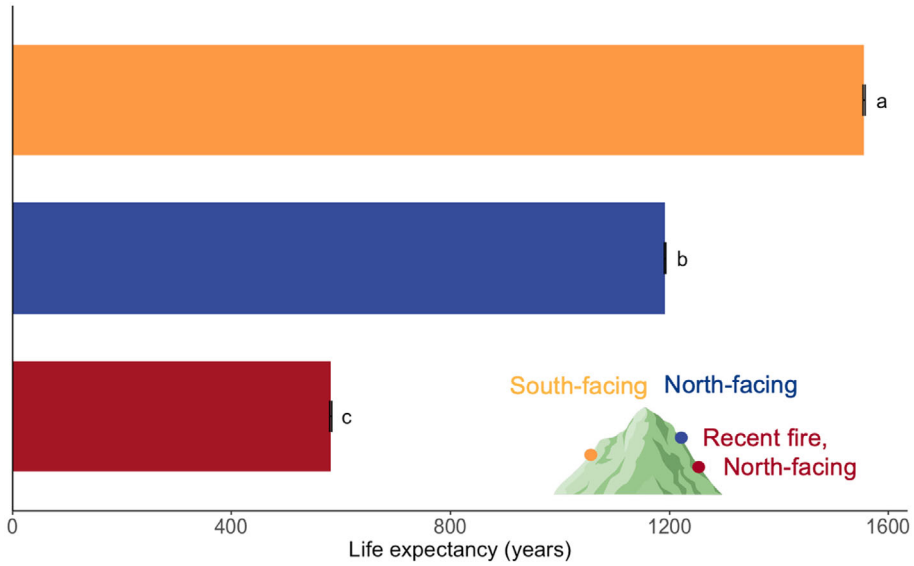


Figure 4. Life expectancy of *Picea mariana* varies significantly across patches exposed to different aspects (South *vs*. North) and fire history. Specifically, in more recently burnt stands, individuals do not live as long as those in a not recently burnt stand of the same height. Letters correspond to a post hoc Tukey test, where groups not sharing the same letter are statistically significantly different at $P < 0.05$.

to increasing fire frequency (Brown & Johnstone, 2012; Johnstone et al., 2020).

The stands modelled on North-facing slopes recently affected by fire produced the shortest passage time and life expectancy, suggesting a trade-off in resilience characteristics. Such conditions may expect to increase their cone production 10-fold (*i.e.*, from 4 m to 5.8 m height; Simpson & Powell, 1981) in less time than stands without recent fire history. This aligns with the finding that a site burnt in 2004 in interior Alaska, stands of *P. mariana* grew faster on burnt than unburnt sites (Tsuyuzaki et al., 2014). While we had hypothesized that such conditions would also support longer life expectancy, we found the opposite. Instead, the finding aligns with the general life history pattern of the fast-slow trade-off, which is well documented in trees (Rüger et al., 2020), and more broadly the Plant Kingdom (Salguero-Gómez et al., 2016). Slower growth may support higher wood density and the mechanical strength to resist breakage/mortality by snowfall or wind (Chave et al., 2009; Elie & Ruel, 2005). Mature stands were found to have greater viable seed rain after fire in Canada's Northwest Territories (Reid et al., 2023), so understanding what conditions support life expectancy in a trade-off with passage time is important. Shorter life expectancy in recently burnt stands may also be explained by phenomena of self-thinning (Reineke, 1933), as has been observed in stands of *P. mariana* in Ontario, Canada (Carleton & Wannamaker, 1987).

In using remote sensing data for ecological monitoring, we must interpret our results in the context of potential data limitations. In our case, tree crowns smaller than 3 m^2 were not included, and the segmentation algorithm struggled to detect small crowns generally. Even so, crowns smaller than 3m^2 are not reliable for LiDAR height tracking with a 1 m^2 resolution CHM because pixel-level noise may obscure height changes relative to larger crowns informed by more pixels. In forests dominated by small crowns, higher resolution CHMs, like LiDAR acquired from drones flown closer to the canopy with high pulse densities, could help overcome this challenge (Savinelli et al., 2024). Also, plot data could be utilized to ground truth crown detection, height change and mortality. Our dataset and subsequent analyses are biased to larger crown trees, meaning that our findings reflect the biology of trees that perhaps have faster passage times or longer life expectancies. Future work to capture more heterogeneity within the population could produce more accurate estimates of passage time and life expectancy, but our findings still reflect the relative impact of environmental conditions on proxies of resilience. Lastly, though we only track a subset of trees ($n \sim 42{,}800$ in 5.5 km^2), utilizing LiDAR allows for replication and spatial coverage to examine the role of multiple environmental variables at a scale that would not be possible with field plot data alone.

Incorporating recruitment data into our LiDAR-parameterized IPMs will further inform our

 © 2026 The Author(s). *Remote Sensing in Ecology and Conservation* published by John Wiley & Sons Ltd on behalf of Zoological Society of London.

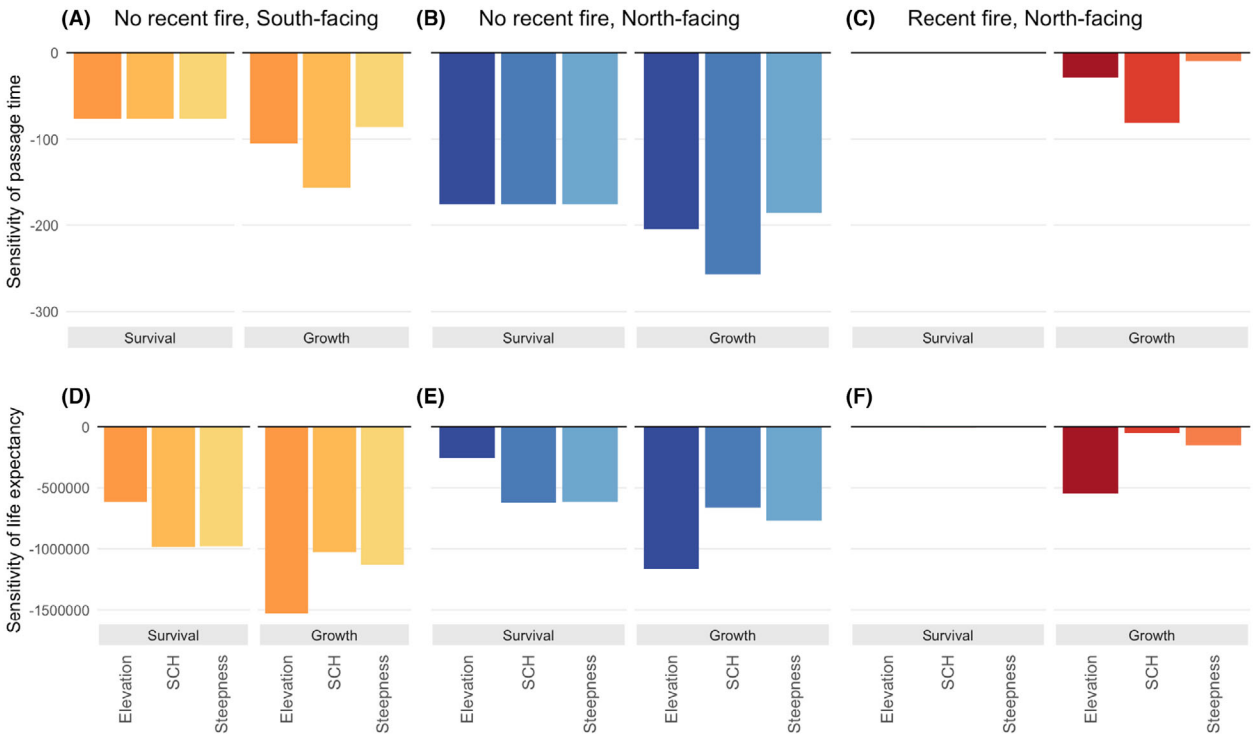


Figure 5. Passage time and life expectancy of *Picea mariana* under the three considered environmental conditions vary in sensitivity to the three environmental drivers: elevation, surrounding canopy height (SCH), and steepness, in both the vital rates of survival and growth. The environmental conditions modelled are: No recent fire, South-facing (A and D); No recent fire, North-facing (B and E); Recent fire, North-facing (C and F). All three environmental conditions have a negative sensitivity to all environmental drivers via contributions of both survival and growth for both passage time and life expectancy. The environmental conditions with the highest sensitivity to any perturbation in environmental drivers for passage time are no recent fire on a North-facing slope (Panel B), while the environmental conditions with the highest sensitivity to any perturbation in environmental drivers for life expectancy are no recent fire on a South-facing slope (Panel D). Negative sensitivity means that when the environmental driver (elevation, SCH, steepness) is increased by a small amount, the passage time/life expectancy decreases. Shorter passage times could result from an increase in survival and an increase in growth. For example, in the case of passage time, a negative sensitivity to an environmental parameter via the contribution of growth refers to a faster growth rate as that would reduce passage time. In the case of life expectancy, a negative sensitivity to an environmental parameter via the contribution of survival refers to lower survival probability as that would reduce life expectancy.

understanding of long-term indicators of resilience of forests. To do so, one would need to estimate reproduction of established individuals as well as the survival and growth of seedlings to the threshold of 4 m height, where LiDAR products can better detect canopy trees (Cao et al., 2023; Dalponte & Coomes, 2016). Importantly though, being taller is not required for black spruce to produce cones, though taller individuals bear more cones (Simpson & Powell, 1981). With fecundity well parameterized in IPMs, one can then also quantify resistance (the lowest the population density reaches post-disturbance) and amplification (the largest the population density reaches post-disturbance), key components, together with recovery time, of demographic resilience (Capdevila et al., 2020). The integration of multi-sensed, multiplatform data acquisition techniques and pertinent *in situ* validation paints an exciting future at the interface of novel technologies and ecological monitoring in forests (Qi et al., 2025; Rosen et al., 2025).

The resilience of forests to anthropogenic disturbances depends on the environmental conditions to which populations have become adapted for survival and growth (Ibáñez et al., 2019). Our analyses reveal that life history traits that aid disturbance recovery, including shorter passage time to heights of higher reproductive viability and longer life expectancy, are mediated by elevation, SCH and slope steepness. Our pipeline integrates hyperspectral-based species maps and LiDAR-derived tree heights, increasing the power of population dynamics models to observe across environmental variation. In combining demographic and environmental data, including LiDAR-derived estimates for larger individual trees, we can better understand global forest trends. We encourage the research community to apply our pipeline to

© 2026 The Author(s). *Remote Sensing in Ecology and Conservation* published by John Wiley & Sons Ltd on behalf of Zoological Society of London.

understand other environmental threats where appropriate remote sensing data are available.

Acknowledgements

We thank R. Battison for LiDAR segmentation and height tracking code, and B. Weinstein and colleagues and F. Fischer for sharing data products of species crown maps and digital surface models respectively. J.M. was supported in part by the Mike Soper Bursary Fund from the Department of Biology at the University of Oxford. We thank the members of the SalGo team and Selva lab for their input in the early stages of development of this project. AR was supported by the Oxford BBSRC DTP studentship (BB/T008784/1) in RSG's lab. RSG was supported by a NERC Pushing the Frontiers grant (NE/X013766/1). The National Ecological Observatory Network (NEON) is a program sponsored by the U.S. National Science Foundation and operated under cooperative agreement by Battelle. Data used in this research were obtained through NEON Research Support Services.

Author Contributions

Jessica McLean: Conceptualization; methodology; formal analysis; visualization; writing – original draft; writing – review and editing; validation; investigation; data curation. **Tommaso Jucker:** Conceptualization; supervision. **Alice Rosen:** Writing – review and editing; visualization. **Sean M. McMahon:** Writing – review and editing; supervision. **Roberto Salguero-Gómez:** Supervision; resources; project administration; writing – review and editing; writing – original draft; conceptualization; methodology; validation; formal analysis; funding acquisition.

Authors' Contribution Statement

JMM, RSG and TJ conceived the ideas and designed methodology; JMM sourced the data and analysed the data; RSG produced R scripts for the demographic modelling and AR and JMM adapted them; JMM led the first draft of the manuscript under the guidance of RSG; All authors contributed critically to the drafts and gave final approval for publication.

Data Accessibility

For the LiDAR-derived digital surface models, the processing pipeline and data products can be found in Fischer et al. (2024). For the hyperspectral-based species map, the processing pipeline and data products can be found in Weinstein et al. (2024). All other data and code used for tree segmentation, constructing the IPMs, and subsequent analyses are hosted on GitHub and can be accessed here: https://github.com/canoeonthelake/hyperspec_map_and_lidar_to_ipm.

Data Availability Statement

The data that supports the findings of this study are available in the supplementary material of this article.

References

Barks, P., Buss, D., Capdevila, P., Caswell, H., Che-Castaldo, J.P., Hinrichsen, R.A., et al. (2023) *Rage: Life history metrics from matrix population models*. https://cran.r-project.org/web/packages/Rage/index.html

Battison, R., Prober, S.M., Zdunic, K., Jackson, T.D., Fischer, F.J. & Jucker, T. (2024) Tracking tree demography and forest dynamics at scale using remote sensing. *New Phytologist*, **244** (6), 2251–2266. https://doi.org/10.1111/nph.20199

Beese, L., Dalponte, M., Asner, G.P., Coomes, D.A. & Jucker, T. (2022) Using repeat airborne LiDAR to map the growth of individual oil palms in Malaysian Borneo during the 2015–16 El Niño. *International Journal of Applied Earth Observation and Geoinformation*, **115**, 103117. https://doi.org/10.1016/j.jag.2022.103117

Bialic-Murphy, L., McElderry, R.M., Esquivel-Muelbert, A., van den Hoogen, J., Zuidema, P.A. et al. (2024) The pace of life for forest trees. *Science*, **386**(6717), 92–98. https://doi.org/10.1126/science.adk9616

Brockerhoff, E.G., Barbaro, L., Castagneyrol, B., Forrester, D.I., Gardiner, B., González-Olabarria, J.R. et al. (2017) Forest biodiversity, ecosystem functioning and the provision of ecosystem services. *Biodiversity and Conservation*, **26**(13), 3005–3035. https://doi.org/10.1007/s10531-017-1453-2

Brown, C.D. & Johnstone, J.F. (2012) Once burned, twice shy: repeat fires reduce seed availability and alter substrate constraints on *Picea mariana* regeneration. *Forest Ecology and Management*, **266**, 34–41. https://doi.org/10.1016/j.foreco.2011.11.006

Buma, B., Hayes, K., Weiss, S. & Lucash, M. (2022) Short-interval fires increasing in the Alaskan boreal forest as fire self-regulation decays across forest types. *Scientific Reports*, **12**(1), 4901. https://doi.org/10.1038/s41598-022-08912-8

Canelles, Q., Aquilué, N., James, P.M.A., Lawler, J. & Brotons, L. (2021) Global review on interactions between insect pests and other forest disturbances. *Landscape Ecology*, **36**(4), 945–972. https://doi.org/10.1007/s10980-021-01209-7

Cao, Y., Ball, J.G.C., Coomes, D.A., Steinmeier, L., Knapp, N., Wilkes, P. et al. (2023) Benchmarking airborne laser scanning tree segmentation algorithms in broadleaf forests shows high accuracy only for canopy trees. *International Journal of Applied Earth Observation and Geoinformation*, **123**, 103490. https://doi.org/10.1016/j.jag.2023.103490

 © 2026 The Author(s). *Remote Sensing in Ecology and Conservation* published by John Wiley & Sons Ltd on behalf of Zoological Society of London.

Capdevila, P., Stott, I., Beger, M. & Salguero-Gómez, R. (2020) Towards a comparative framework of demographic resilience. *Trends in Ecology & Evolution*, **35**(9), 776–786. https://doi.org/10.1016/j.tree.2020.05.001

Capdevila, P., Stott, I., Cant, J., Beger, M., Rowlands, G., Grace, M. et al. (2022) Life history mediates the trade-offs among different components of demographic resilience. *Ecology Letters*, **25**(6), 1566–1579. https://doi.org/10.1111/ele.14004

Carleton, T.J. & Wannamaker, B.A. (1987) Mortality and self-thinning in postfire black spruce. *Annals of Botany*, **59** (6), 621–628. https://doi.org/10.1093/oxfordjournals.aob.a087358

Cavendar-Bares, J., Gamon, J.A. & Townsend, P.A. (2020) *Remote sensing of plant biodiversity*. Cham: Springer Nature. https://library.oapen.org/handle/20.500.12657/39986

Chapin, F.S., Oswood, M.W., Van Cleve, K., Viereck, L.A. & Verbyla, D.L. (2006) *Alaska's changing boreal forest*. Oxford: Oxford University Press. https://doi.org/10.1093/oso/9780195154313.001.0001

Chave, J., Coomes, D., Jansen, S., Lewis, S.L., Swenson, N.G. & Zanne, A.E. (2009) Towards a worldwide wood economics spectrum. *Ecology Letters*, **12**(4), 351–366. https://doi.org/10.1111/j.1461-0248.2009.01285.x

Choi, D.H., LaRue, E.A., Atkins, J.W., Foster, J.R., Matthes, J.H., Fahey, R.T. et al. (2023) Short-term effects of moderate severity disturbances on forest canopy structure. *Journal of Ecology*, **111**(9), 1866–1881. https://doi.org/10.1111/1365-2745.14145

Clark, J.S. (2003) Uncertainty and variability in demography and population growth: a hierarchical approach. *Ecology*, **84** (6), 1370–1381.

Cobb, R.C., Ruthrof, K.X., Breshears, D.D., Lloret, F., Aakala, T., Adams, H.D. et al. (2017) Ecosystem dynamics and management after forest die-off: a global synthesis with conceptual state-and-transition models. *Ecosphere*, **8**(12), e02034. https://doi.org/10.1002/ecs2.2034

Coulson, T. (2012) Integral projections models, their construction and use in posing hypotheses in ecology. *Oikos*, **121**(9), 1337–1350. https://doi.org/10.1111/j.1600-0706.2012.00035.x

Cronan, J., McKenzie, D. & Olson, D. (2012) *Fire regimes of the Alaskan boreal forest. Gen. Tech. Rep. PNW-GTR-XXX*. Portland, OR: U.S. Department of Agriculture, Forest Service, Pacific Northwest Research Station. https://www.frames.gov/documents/alaska/fire_history/cronan_mckenzie_olson_2011_FireRegimesOfTheAlaskanBorealForest_gtr-DRAFT.pdf

Cushman, K.C., Burley, J.T., Imbach, B., Saatchi, S.S., Silva, C.E., Vargas, O. et al. (2021) Impact of a tropical forest blowdown on aboveground carbon balance. *Scientific Reports*, **11**(1), 11279. https://doi.org/10.1038/s41598-021-90576-x

Dalponte, M. & Coomes, D.A. (2016) Tree-centric mapping of forest carbon density from airborne laser scanning and hyperspectral data. *Methods in Ecology and Evolution*, **7**(10), 1236–1245. https://doi.org/10.1111/2041-210X.12575

Dearborn, K.D., Wallace, C.A., Patankar, R. & Baltzer, J.L. (2021) Permafrost thaw in boreal peatlands is rapidly altering forest community composition. *Journal of Ecology*, **109**(3), 1452–1467. https://doi.org/10.1111/1365-2745.13569

Drobyshev, I., Gewehr, S., Berninger, F. & Bergeron, Y. (2013) Species specific growth responses of black spruce and trembling aspen may enhance resilience of boreal forest to climate change. *Journal of Ecology*, **101**(1), 231–242. https://doi.org/10.1111/1365-2745.12007

Duncanson, L. & Dubayah, R. (2018) Monitoring individual tree-based change with airborne lidar. *Ecology and Evolution*, **8**(10), 5079–5089. https://doi.org/10.1002/ece3.4075

Easterling, M., Ellner, S. & Dixon, P. (2000) Size-specific sensitivity: applying a new structured population model. *Ecology*, **81**, 694–708. https://doi.org/10.2307/177370

Elie, J.-G. & Ruel, J.-C. (2005) Windthrow hazard modelling in boreal forests of black spruce and jack pine. *Canadian Journal of Forest Research*, **35**(11), 2655–2663. https://doi.org/10.1139/x05-189

Ellner, S.P. & Rees, M. (2006) Integral projection models for species with complex demography. *The American Naturalist*, **167**(3), 410–428. https://doi.org/10.1086/499438

Ellner, S.P., Childs, D.Z. & Rees, M. (2016) Data-driven modelling of structured populations: a practical guide to the integral projection model. In: *Lecture notes on mathematical modelling in the life sciences*. Cham: Springer International Publishing. https://doi.org/10.1007/978-3-319-28893-2

Fassnacht, F.E., White, J.C., Wulder, M.A. & Næsset, E. (2024) Remote sensing in forestry: current challenges, considerations and directions. *Forestry: An International Journal of Forest Research*, **97**(1), 11–37. https://doi.org/10.1093/forestry/cpad024

Fischer, F.J., Jackson, T., Vincent, G. & Jucker, T. (2024) Robust characterisation of forest structure from airborne laser scanning—a systematic assessment and sample workflow for ecologists. *Methods in Ecology and Evolution*, **15**(10), 1873–1888. https://doi.org/10.1111/2041-210X.14416

Fischer, F.J., Morgan, B., Jackson, T., Chave, J., Coomes, D., Cushman, K.C. et al (2025) *The global canopy atlas: analysis-ready maps of 3D structure for the world's woody ecosystems*.p.2025.08.31.673375. BioRxiv [Preprint]. https://doi.org/10.1101/2025.08.31.673375

Fryer, J.L. (2014) Picea mariana. In: *Fire Effects Information System, [Online]*. U.S. Department of Agriculture, Forest Service, Rocky Mountain Research Station, Fire Sciences Laboratory (Producer). Available: https://www.fs.usda.gov/database/feis/plants/tree/picmar/all.html [2026, January 14].

Hammond, W.M., Williams, A.P., Abatzoglou, J.T., Adams, H.D., Klein, T., López, R. et al. (2022) Global field observations of tree die-off reveal hotter-drought fingerprint for Earth's forests. *Nature Communications*, **13**(1), 1761. https://doi.org/10.1038/s41467-022-29289-2

© 2026 The Author(s). *Remote Sensing in Ecology and Conservation* published by John Wiley & Sons Ltd on behalf of Zoological Society of London.

Hart, S.A. & Chen, H.Y.H. (2006) Understory vegetation dynamics of north American boreal forests. *Critical Reviews in Plant Sciences*, **25**(4), 381–397. https://doi.org/10.1080/07352680600819286

Hawryło, P., Socha, J., Wężyk, P., Ochał, W., Krawczyk, W., Miszczyszyn, J. et al. (2024) How to adequately determine the top height of forest stands based on airborne laser scanning point clouds? *Forest Ecology and Management*, **551**, 121528. https://doi.org/10.1016/j.foreco.2023.121528

Hijmans R.J. Bivand R. Dyba K. Pebesma E. Sumner M.D. (2024) terra: spatial data analysis. https://cran.r-project.org/web/packages/terra/index.html

Hinzman, L.D., Fukuda, M., Sandberg, D.V., Chapin, F.S., III & Dash, D. (2003) FROSTFIRE: An experimental approach to predicting the climate feedbacks from the changing boreal fire regime. *Journal of Geophysical Research-Atmospheres*, **108**(D1), FFR 9-1–FFR 9-6. https://doi.org/10.1029/2001JD000415

Hogan, J.A., Domke, G.M., Zhu, K., Johnson, D.J. & Lichstein, J.W. (2024) Climate change determines the sign of productivity trends in US forests. *Proceedings of the National Academy of Sciences*, **121**(4), e2311132121. https://doi.org/10.1073/pnas.2311132121

Holling, C.S. (1973) Resilience and stability of ecological systems. *Annual Review of Ecology and Systematics*, **4**, 1–23.

Ibáñez, I., Acharya, K., Juno, E., Karounos, C., Lee, B.R., McCollum, C. et al. (2019) Forest resilience under global environmental change: do we have the information we need? A systematic review. *PLoS One*, **14**(9), e0222207. https://doi.org/10.1371/journal.pone.0222207

Johnstone, J.F., Celis, G., Chapin, F.S., III, Hollingsworth, T.N., Jean, M. & Mack, M.C. (2020) Factors shaping alternate successional trajectories in burned black spruce forests of Alaska. *Ecosphere*, **11**(5), e03129. https://doi.org/10.1002/ecs2.3129

Jones, O.R., Barks, P., Stott, I., James, T.D., Levin, S., Petry, W.K. et al. (2022) Rcompadre and rage—two R packages to facilitate the use of the COMPADRE and COMADRE databases and calculation of life-history traits from matrix population models. *Methods in Ecology and Evolution*, **13**(4), 770–781. https://doi.org/10.1111/2041-210X.13792

Jucker, T. (2022) Deciphering the fingerprint of disturbance on the three-dimensional structure of the world's forests. *New Phytologist*, **233**(2), 612–617. https://doi.org/10.1111/nph.17729

Jucker, T., Caspersen, J., Chave, J., Antin, C., Barbier, N., Bongers, F. et al. (2017) Allometric equations for integrating remote sensing imagery into forest monitoring programmes. *Global Change Biology*, **23**(1), 177–190. https://doi.org/10.1111/gcb.13388

Krause, C. & Lemay, A. (2023) Development and growth of young black spruce (*Picea mariana*) trees under two different hydrological conditions. *Forest Ecology and Management*, **541**, 121083. https://doi.org/10.1016/j.foreco.2023.121083

Kunstler, G., Guyennon, A., Ratcliffe, S., Rüger, N., Ruiz-Benito, P., Childs, D.Z. et al. (2021) Demographic performance of European tree species at their hot and cold climatic edges. *Journal of Ecology*, **109**(2), 1041–1054. https://doi.org/10.1111/1365-2745.13533

Ma, Q., Su, Y., Niu, C., Ma, Q., Hu, T., Luo, X. et al. (2023) Tree mortality during long-term droughts is lower in structurally complex forest stands. *Nature Communications*, **14**(1), 7467. https://doi.org/10.1038/s41467-023-43083-8

MacDonald, G.M., Larsen, C.P.S., Szeicz, J.M. & Moser, K.A. (1991) The reconstruction of boreal forest fire history from lake sediments: a comparison of charcoal, pollen, sedimentological, and geochemical indices. *Quaternary Science Reviews*, **10**(1), 53–71. https://doi.org/10.1016/0277-3791(91)90030-X

Makowski, D., Lüdecke, D., Patil, I., Thériault, R., Ben-Shachar, M.S., Wiernik, B.M., Siegel, R. & Bock, C. (2025) report: Automated Reporting of Results and Statistical Models. https://cran.r-project.org/web/packages/report/index.html

May, R.M. (1977) Thresholds and breakpoints in ecosystems with a multiplicity of stable states. *Nature*, **269**(5628), 471–477. https://doi.org/10.1038/269471a0

Maynard, D.S., Bialic-Murphy, L., Zohner, C.M., Averill, C., van den Hoogen, J., Ma, H. et al. (2022) Global relationships in tree functional traits. *Nature Communications*, **13**(1), 3185. https://doi.org/10.1038/s41467-022-30888-2

McMahon, S.M., Parker, G.G. & Miller, D.R. (2010) Evidence for a recent increase in forest growth. *Proceedings of the National Academy of Sciences*, **107**(8), 3611–3615. https://doi.org/10.1073/pnas.0912376107

Melvin, A.M., Mack, M.C., Johnstone, J.F., McGuire, A.D., Genet, H. & Schuur, E.A.G. (2015) Differences in ecosystem carbon distribution and nutrient cycling linked to forest tree species composition in a mid-successional boreal forest. *Ecosystems*, **18**(8), 1472–1488. https://doi.org/10.1007/s10021-015-9912-7

Merow, C., Dahlgren, J.P., Metcalf, C.J.E., Childs, D.Z., Evans, M.E.K., Jongejans, E. et al. (2014) Advancing population ecology with integral projection models: a practical guide. *Methods in Ecology and Evolution*, **5**(2), 99–110. https://doi.org/10.1111/2041-210X.12146

Metcalf, C.J.E., Horvitz, C.C., Tuljapurkar, S. & Clark, D.A. (2009) A time to grow and a time to die: a new way to analyze the dynamics of size, light, age, and death of tropical trees. *Ecology*, **90**(10), 2766–2778. https://doi.org/10.1890/08-1645.1

Metcalf, C.J.E., McMahon, S.M., Salguero-Gómez, R. & Jongejans, E. (2013) IPMpack: an R package for integral projection models. *Methods in Ecology and Evolution*, **4**(2), 195–200. https://doi.org/10.1111/2041-210x.12001

 © 2026 The Author(s). *Remote Sensing in Ecology and Conservation* published by John Wiley & Sons Ltd on behalf of Zoological Society of London.

Mo, L., Zohner, C.M., Reich, P.B., Liang, J., de Miguel, S., Nabuurs, G.J. et al. (2023) Integrated global assessment of the natural forest carbon potential. *Nature*, **624**(7990), 92–101. https://doi.org/10.1038/s41586-023-06723-z

Morin, X., Fahse, L., Jactel, H., Scherer-Lorenzen, M., García-Valdés, R. & Bugmann, H. (2018) Long-term response of forest productivity to climate change is mostly driven by change in tree species composition. *Scientific Reports*, **8**(1), 5627. https://doi.org/10.1038/s41598-018-23763-y

Morris, W.F. & Doak, D.F. (2002) *Quantitative conservation biology: theory and practice of population viability analysis*. Sunderland: Sinauer Associates. https://cir.nii.ac.jp/crid/1130282270295869696

Nath, B. & Ni-Meister, W. (2021) The interplay between canopy structure and topography and its impacts on seasonal variations in surface reflectance patterns in the boreal region of Alaska—implications for surface radiation budget. *Remote Sensing*, **13**, 3108. https://doi.org/10.3390/rs13163108

Needham, J., Merow, C., Butt, N., Malhi, Y., Marthews, T.R., Morecroft, M. et al. (2016) Forest community response to invasive pathogens: the case of ash dieback in a British woodland. *Journal of Ecology*, **104**(2), 315–330. https://doi.org/10.1111/1365-2745.12545

Needham, J., Merow, C., Chang-Yang, C.-H., Caswell, H. & McMahon, S.M. (2018) Inferring forest fate from demographic data: from vital rates to population dynamic models. *Proceedings of the Royal Society B: Biological Sciences*, **285**(1874), 20172050. https://doi.org/10.1098/rspb.2017.2050

NEON (National Ecological Observatory Network). (2025a) Discrete return LiDAR point cloud (DP1.30003.001). Dataset accessed from https://data.neonscience.org/data-products/DP1.30003.001/RELEASE-2025 on October 23, 2025a. https://doi.org/10.48443/jyb5-g533

NEON (National Ecological Observatory Network). (2025b) High-resolution orthorectified camera imagery (DP1.30010.001). Dataset accessed from https://data.neonscience.org/data-products/DP1.30010.001/RELEASE-2025 on October 16, 2025b. https://doi.org/10.48443/f8dg-8w18

NEON (National Ecological Observatory Network). (2025c) Vegetation structure (DP1.10098.001). Dataset accessed from https://data.neonscience.org/data-products/DP1.10098.001/RELEASE-2025 on October 16, 2025c. https://doi.org/10.48443/653k-mf13

Nicoll, B.C., Achim, A., Mochan, S. & Gardiner, B.A. (2005) Does steep terrain influence tree stability? A field investigation. *Canadian Journal of Forest Research*, **35**(10), 2360–2367. https://doi.org/10.1139/x05-157

Ohse, B., Compagnoni, A., Farrior, C.E., McMahon, S.M., Salguero-Gómez, R., Rüger, N. et al. (2023) Demographic synthesis for global tree species conservation. *Trends in Ecology & Evolution*, **38**(6), 579–590. https://doi.org/10.1016/j.tree.2023.01.013

Palm, E.C., Suitor, M.J., Joly, K., Herriges, J.D., Kelly, A.P., Hervieux, D. et al. (2022) Increasing fire frequency and severity will increase habitat loss for a boreal forest indicator species. *Ecological Applications*, **32**(3), e2549. https://doi.org/10.1002/eap.2549

Pebesma, E. (2018) Simple features for R: standardized support for spatial vector data. *The R Journal*, **10**(1), 439–446.

Pimm, S.L. (1984) The complexity and stability of ecosystems. *Nature*, **307**(5949), 321–326. https://doi.org/10.1038/307321a0

Qi, M., Gadd, M., Martini, D.D., Davis, K., Xiong, B., Rosen, A., et al. (2025) *Biodiversity research requires more motors in the mud, air and water*. EcoEvoRxiv [Preprint]. https://doi.org/10.32942/X22H0D

R Core Team. (2023) *R: a language and environment for statistical computing*. Vienna, Australia: R Foundation for Statistical Computing. https://www.r-project.org/

Rees, M., Childs, D.Z. & Ellner, S.P. (2014) Building integral projection models: a user's guide. *Journal of Animal Ecology*, **83**(3), 528–545. https://doi.org/10.1111/1365-2656.12178

Reid, K.A., Day, N.J., Alfaro-Sánchez, R., Johnstone, J.F., Cumming, S.G., Mack, M.C. et al. (2023) Black spruce (*Picea mariana*) seed availability and viability in boreal forests after large wildfires. *Annals of Forest Science*, **80**(1), 4. https://doi.org/10.1186/s13595-022-01166-4

Reineke, L.H. (1933) Perfecting a stand-density index for even-aged forest. *Journal of Agricultural Research*, **46**, 627–638.

Roces-Díaz, J.V., Santín, C., Martínez-Vilalta, J. & Doerr, S.H. (2022) A global synthesis of fire effects on ecosystem services of forests and woodlands. *Frontiers in Ecology and the Environment*, **20**(3), 170–178. https://doi.org/10.1002/fee.2349

Rosen A. Battison R. Hernández C.M. Spacey O. McLean J. Prober S. et al. (2025) Modelling forest dynamics using integral projection models (IPMs) and repeat LiDAR. BioRxiv. https://doi.org/10.1101/2025.01.06.631514

Roussel J.-R. (2025) lidR: Aiirborne LiDAR data manipulation and visualization forrborne LiDAR data manipulation and visualization for forestry applications. https://cran.r-project.org/web/packages/lidR/index.html

Roussel, J.-R., Auty, D., Coops, N.C., Tompalski, P., Goodbody, T.R.H., Meador, A.S. et al. (2020) lidR: an R package for analysis of airborne laser scanning (ALS) data. *Remote Sensing of Environment*, **251**, 112061. https://doi.org/10.1016/j.rse.2020.112061

Rüger, N., Condit, R., Dent, D.H., DeWalt, S.J., Hubbell, S.P., Lichstein, J.W. et al. (2020) Demographic trade-offs predict tropical forest dynamics. *Science*, **368**, 165–168. https://doi.org/10.1126/science.aaz4797

Salguero-Gómez, R. & Gamelon, M. (2021) *Demographic methods across the tree of life*. Oxford, New York: Oxford University Press.

Salguero-Gómez, R., Jones, O.R., Archer, C.R., Buckley, Y.M., Che-Castaldo, J., Caswell, H. et al. (2015) The compadre

© 2026 The Author(s). *Remote Sensing in Ecology and Conservation* published by John Wiley & Sons Ltd on behalf of Zoological Society of London.

plant matrix database: an open online repository for plant demography. *Journal of Ecology*, **103**(1), 202–218. https://doi.org/10.1111/1365-2745.12334

Salguero-Gómez, R., Jones, O.R., Jongejans, E., Blomberg, S.P., Hodgson, D.J., Mbeau-Ache, C. et al. (2016) Fast–slow continuum and reproductive strategies structure plant life-history variation worldwide. *Proceedings of the National Academy of Sciences*, **113**(1), 230–235. https://doi.org/10.1073/pnas.1506215112

Savinelli, B., Tagliabue, G., Vignali, L., Garzonio, R., Gentili, R., Panigada, C. et al. (2024) Integrating drone-based LiDAR and multispectral data for tree monitoring. *Drones*, **8**(12), 744. https://doi.org/10.3390/drones8120744

Scholl, V.M., Cattau, M.E., Joseph, M.B. & Balch, J.K. (2020) Integrating National Ecological Observatory Network (NEON) airborne remote sensing and in-situ data for optimal tree species classification. *Remote Sensing*, **12**(9), 1414. https://doi.org/10.3390/rs12091414

Simpson, J.D. & Powell, G.R. (1981) Some factors influencing cone production on young black spruce in New Brunswick. *Forestry Chronicle*, **57**(6), 267–269. https://doi.org/10.5558/tfc57267-6

Splawinski, T.B., Boucher, Y., Bouchard, M., Greene, D.F., Gauthier, S., Auger, I. et al. (2022) Factors influencing black spruce reproductive potential in the northern boreal forest of Quebec. *Canadian Journal of Forest Research*, **52**(12), 1499–1512. https://doi.org/10.1139/cjfr-2022-0092

Stovall, A.E.L., Shugart, H. & Yang, X. (2019) Tree height explains mortality risk during an intense drought. *Nature Communications*, **10**(1), 4385. https://doi.org/10.1038/s41467-019-12380-6

Thorogood, R., Mustonen, V., Aleixo, A., Aphalo, P.J., Asiegbu, F.O. et al. (2023) Understanding and applying biological resilience, from genes to ecosystems. *npj Biodiversity*, **2**(1), 1–13. https://doi.org/10.1038/s44185-023-00022-6

Tollefson, J. (2024) You're not imagining it: extreme wildfires are now more common. *Nature*. https://doi.org/10.1038/d41586-024-02071-8

Tsuyuzaki, S., Narita, K., Sawada, Y. & Kushida, K. (2014) The establishment patterns of tree seedlings are determined immediately after wildfire in a black spruce (Picea mariana) forest. *Plant Ecology*, **215**(3), 327–337. https://doi.org/10.1007/s11258-014-0303-5

Van Cleve, K., Chapin, F.S., Flanagan, P.W., Viereck, L.A., Dyrness, C.T., Billings, W.D. et al. (1986) Forest ecosystems in the Alaskan taiga: a synthesis of structure and function. In: Van Cleve, K., Chapin, F.S., III, Flanagan, P.W., Viereck, L.A. & Dyrness, C.T. (Eds.) *Ecological Studies*. New York, NY: Springer. https://doi.org/10.1007/978-1-4612-4902-3

Viglas, J.N., Brown, C.D. & Johnstone, J.F. (2013) Age and size effects on seed productivity of northern black spruce. *Canadian Journal of Forest Research*, **43**(6), 534–543. https://doi.org/10.1139/cjfr-2013-0022

Weinstein, B., Marconi, S., Zare, A., Bohlman, S., Graves, S., Singh, A., et al. (2020) NEON tree crowns dataset. https://doi.org/10.5281/zenodo.3765872

Weinstein, B.G., Marconi, S., Zare, A., Bohlman, S.A., Singh, A., Graves, S.J., et al. (2024) *Individual canopy tree species maps for the National Ecological Observatory Network*.p.2023.10.25.563626. https://doi.org/10.1101/2023.10.25.563626

Whitman, E., Parisien, M.-A., Thompson, D.K. & Flannigan, M.D. (2019) Short-interval wildfire and drought overwhelm boreal forest resilience. *Scientific Reports*, **9**(1), 18796. https://doi.org/10.1038/s41598-019-55036-7

Zambrano, J. & Salguero-Gómez, R. (2014) Forest fragmentation alters the population dynamics of a late-successional tropical tree. *Biotropica*, **46**(5), 556–564. https://doi.org/10.1111/btp.12144

Zuleta, D., Arellano, G., Muller-Landau, H.C., McMahon, S.M., Aguilar, S., Bunyavejchewin, S. et al. (2022) Individual tree damage dominates mortality risk factors across six tropical forests. *New Phytologist*, **233**(2), 705–721. https://doi.org/10.1111/nph.17832

Supporting Information

Additional supporting information may be found online in the Supporting Information section at the end of the article.

Data S1.
Data S2.

 © 2026 The Author(s). *Remote Sensing in Ecology and Conservation* published by John Wiley & Sons Ltd on behalf of Zoological Society of London.